Finite Temperature Quasicontinuum: Molecular Dynamics without all the Atoms

L. Dupuy
Lawrence Livermore National Laboratory, L-415, Livermore, CA 94551, USA

E. B. Tadmor
Faculty of Mechanical Engineering, Technion – Israel Institute of Technology, 32000 Haifa, ISRAEL

R. E. Miller
Department of Mechanical and Aerospace Engineering, Carleton University, Ottawa, CANADA

R. Phillips
Division of Engineering and Applied Science, California Institute of Technology, Pasadena, CA 91125, USA
(Dated: February 4, 2005)

Using a combination of statistical mechanics and finite-element interpolation, we develop a coarse-grained (CG) alternative to molecular dynamics (MD) for crystalline solids at constant temperature. The new approach is significantly more efficient than MD and generalizes earlier work on the quasicontinuum method. The method is validated by recovering equilibrium properties of single crystal Ni as a function of temperature. CG dynamical simulations of nanoindentation reveal a strong dependence on temperature of the critical stress to nucleate dislocations under the indenter.

PACS numbers: 02.70.Ns, 02.70.Dh, 62.25.+g, 68.60.Dv, 83.50.-v

Many processes involving the physics and chemistry of materials result from microscopic interactions between the constituent atoms. As a result, molecular dynamics (MD) simulations pervade the literature of a variety of materials-related disciplines. Despite ever-increasing computer power, large-scale atomistic simulations remain computationally demanding, resulting in the continued effort to seek alternatives which permit the examination of larger spatial domains or longer time scales.

An important step in this direction has taken place in recent years with the development of a variety of multiscale methods which combine atomistic simulation with coarse-graining schemes (see [1] for a recent review). These methods exploit the fact that in many cases the critical dynamics may involve a relatively small subset of the entire set of atoms with the remainder of the atoms serving primarily to guarantee appropriate boundary conditions for the region of interest. One example is the quasicontinuum (QC) method, a zero-temperature energy minimization technique, which significantly reduces the total number of degrees of freedom that must be considered when simulating the deformation of crystalline solids [2]. In this method an approximation to the total potential energy is obtained by making use of finite-element constraints to remove atoms where the deformation field varies slowly on the scale of the lattice parameter. An attractive feature of this approach is its "seamlessness" in that the same underlying atomistic model is used in the energy calculations in both the coarse-grained (CG) and fully-atomistic regions.

The aim of this paper is to extend the QC method to treat the dynamics of systems at constant temperature. This procedure is based on ideas drawn from computational statistical mechanics and is tied to the use of the Nosé-Poincaré thermostat. The atomistic regions obey the usual equations of motions at finite temperature leading to an appropriate description of detailed atomic-scale events. On the other hand, in regions not subject to severe deformations, a significant number of degrees of freedom are integrated out assuming local thermal equilibrium. We assess the validity of the method by comparing the temperature dependence of the lattice parameter of the CG system with a fully atomistic model which serves as the gold standard for the method. In addition, we use the method to study the temperature dependence of dislocation nucleation during nanoindentation.

Consider a system of N atoms whose positions are denoted by $\{\mathbf{q}\}$. We assume the potential energy of the system $V(\{\mathbf{q}\})$ can be written as the sum of the energy $E_i(\{\mathbf{q}\})$ of each individual atom i. As shown in Fig. 1, we split the atom population (N atoms) between so-called *representative atoms* (repatoms), characterized by positions $\{\mathbf{q}^r\}$, which are the atoms that we will consider in our simulations and *constrained atoms* with coordinates $\{\mathbf{q}^c\}$. We define N_r as the number of repatoms and we will refer to this system as the CG system. The design criterion for the CG dynamics is the requirement that the CG system behaves as closely as possible to the full system at finite temperature. This raises the question of which metric to use to assess the success of the CG system as a surrogate for the all-atom system. One criterion that we impose is the requirement that the time-average of any observable A (designated as $\bar{A}$) that depends *only* on the positions of the repatoms $\{\mathbf{q}^r\}$ be equal to the time-average that would be found for this observable in a full atomistic and canonical system. Assuming equal-

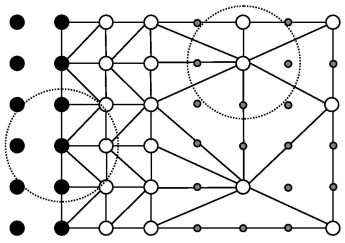

FIG. 1: We split the atom population between *representative atoms* (large circles on the figure) and *constrained atoms* (small gray circles). The average position of the latter are estimated from the position of the former using finite-element interpolation. Among the repatoms, we make a distinction between *non-local* atoms (black circles) whose energy only depends on repatoms (as shown by the dashed circle whose radius equals the cutoff distance of the interatomic potential), and the *local* atoms (white circles) which interact with constrained atoms.

ity of time and ensemble averages, this constraint can be stated as

$$\bar{A}\left(\{\mathbf{q}^r\}\right)_{\mathrm{CG}} = \bar{A}\left(\{\mathbf{q}^r\}\right)_{\mathrm{N,V,T}} = \left\langle A\left(\{\mathbf{q}^r\}\right)\right\rangle_{\mathrm{N,V,T}}, \quad (1)$$

where $\langle A\rangle$ is the ensemble average of A. The Hamiltonian of the canonical CG system is constructed as follows. We first write the potential energy of the complete system as $V\left(\{\mathbf{q}^r\},\{\mathbf{q}^c\}\right)$ with the coordinates divided into the representative and constrained sets. Following [3], we define the CG potential energy as

$$V_{\mathrm{CG}}\left(\{\mathbf{q}^r\},\beta\right) = -\frac{1}{\beta}\ln\int e^{-\beta V\left(\{\mathbf{q}^r\},\{\mathbf{q}^c\}\right)} d\{\mathbf{q}^c\}, \quad (2)$$

where $\beta = 1/k_{\mathrm{B}}T$. This *ansatz* is the mathematical embodiment of our coarse-graining principle. In particular, it guarantees that the repatoms fulfill the injunction implied in Eq. 1. The Hamiltonian of the CG system is

$$H_{\mathrm{CG}}\left(\{\mathbf{q}^r\},\{\mathbf{p}^r\},\beta\right) = \sum_{i=1}^{N_r}\frac{\left(\mathbf{p}_i^r\right)^2}{2m_i^r} + V_{\mathrm{CG}}\left(\{\mathbf{q}^r\},\beta\right),$$

where $\mathbf{p}_i^r = m_i^r\dot{\mathbf{q}}_i^r$ are the momenta of the repatoms and m_i^r are their effective masses. The effective masses are obtained from the conditions that the total mass of the CG system equals that of the full-atom system, $\sum_i m_i^r = Nm$, and that both systems have the same momentum free energy F_p,

$$F_p = -\frac{1}{\beta}\ln\prod_{i=1}^{N_r}\left(\frac{2\pi m_i^r}{\beta h_p^2}\right)^{3/2} = -\frac{1}{\beta}\ln\left(\frac{2\pi m}{\beta h_p^2}\right)^{3N/2},$$

where h_p is an arbitrary constant with dimensions of momentum [4]. These requirements are satisfied identically if $h_p = \sqrt{2\pi m/\alpha\beta}$ and the effective masses are taken to be $m_i^r = \alpha^{n_i-1}m$, where n_i is the number of atoms represented by repatom i and α is obtained from the solution of the equation, $\sum_{i=1}^{N_r}\alpha^{n_i-1} = N$.

While the choice of whether or not an atom should be representative remains *ad-hoc*, it is based upon two criteria. First, the atoms in or directly surrounding the regions of interest should all be representative in order to ensure equations of motion which are the same as those for the full-atom system. Second, the distribution of repatoms in the CG regions should be adapted with the evolving displacement field in order to make the calculation of $V_{\mathrm{CG}}\left(\{\mathbf{q}^r\},\beta\right)$ as accurate as possible.

In order to construct a dynamics for the repatoms which allows for the simulation of systems in contact with a thermal reservoir, we follow Nosé in introducing a virtual *microcanonical* system (N_r+1,V,$\hat{H}_{\mathrm{CG}}$) that will mimic our *canonical* system [5], though now applied to the set of repatoms rather than all of the atoms. For definiteness, we designate the coordinates of the virtual system by $\hat{\cdot}$. In addition, we use a Poincaré time transformation to avoid a distinction between the time $\hat{t}$ governing the virtual system and the real system ($t = \hat{t}$) while maintaining Hamiltonian dynamics [6]. We define the following virtual Hamiltonian

$$\hat{H}_{\mathrm{CG}}\left(\{\hat{\mathbf{q}}^r\},\{\hat{\mathbf{p}}^r\},\hat{s},\hat{p_s}\right) = \hat{s}\left[\sum_{i=1}^{N_r}\frac{\left(\hat{\mathbf{p}}_i^r\right)^2}{2m_i^r\hat{s}^2} + \frac{\hat{p_s}^2}{2Q}\right] + \left[V_{\mathrm{CG}}\left(\{\hat{\mathbf{q}}^r\},\beta\right) + \frac{g}{\beta}\ln s - H_0\right],$$

where $\hat{s}$ and $\hat{p}_s$ are respectively the position and momentum of an effective mass Q associated with the thermal reservoir. $\hat{\mathbf{q}}^r$ and $\hat{\mathbf{p}}^r$ are the positions and momenta of the repatoms in the virtual system with the effective masses remaining unchanged. H_0 is a constant which is chosen such that $\hat{H}_{\mathrm{CG}}$ equals 0 at time $\hat{t} = 0$. The value of g is taken as $N_r d$ (where d is the number of dimensions of the system). Following Nosé's original demonstration [5], it can be shown that this virtual microcanonical system (N_r+1,V,$\hat{H}_{\mathrm{CG}}$) is equivalent to our CG canonical system by using the following relations, $\mathbf{q}_i^r = \hat{\mathbf{q}}_i^r$, $\mathbf{p}_i^r = \hat{\mathbf{p}}_i^r/s$. Just as is found in the all-atom analog of the current discussion, it can be shown that averages in the microcanonical N_r+1 degrees of freedom system implies canonical averages for the nodal degrees of freedom as

$$\bar{A}\left(\{\hat{\mathbf{q}}^r\}\right)_{\mathrm{N_r+1,V,\hat{H}}} = \bar{A}\left(\{\mathbf{q}^r\}\right)_{\mathrm{N,V,T}} = \left\langle A\left(\{\mathbf{q}^r\}\right)\right\rangle_{\mathrm{N,V,T}}.$$

This ensures that Eq. 1 is respected.

Equations of motions can now be derived from the Hamiltonian $\hat{H}_{\mathrm{CG}}$. These equations can be integrated in turn using a time-reversible and area-preserving algorithm [7]. It should be noted that the resulting equations of motion for atoms in fully-refined regions are identical to those of a full atomistic and microcanonical simulation with an additional damping/accelerator term which maintains the system at the correct temperature.

Although the description given above is formally complete, we must still address the question of how to implement these ideas numerically. Here we appeal to the

QC formalism [2] to describe the configuration of the system and to compute the CG potential $V_{\rm CG}\left(\{\mathbf{q}^r\},\beta\right)$ as given by Eq. 2. As in previous work, we lay down a mesh between the repatoms and decompose them into two sets as shown in Fig. 1. The *non-local atoms* (NL) are the atoms located in fully-refined regions which do not interact with any constrained atoms. Their individual contribution $E_i\left(\{\mathbf{q}^r\}\right)$ to the CG potential can be calculated exactly based on the positions of the surrounding repatoms as one would do in regular MD.

On the other hand, *local atoms* interact with the constrained atoms in their vicinity. In principle, their contribution cannot be considered individually and requires tedious integrations over all the possible positions of the constrained atoms. However, we can take advantage of the smoothness of the strain field in the CG regions and invoke the *Cauchy-Born rule* [2]. The CG potential energy in Eq. 2 can then be decomposed into a non-local part and a local part written as a sum over CG elements,

$$V_{\rm CG}\left(\{\mathbf{q}^r\},\beta\right)=\sum_{i\in{\rm NL}}E_i-\sum_e\frac{1}{\beta}\ln\int e^{-\beta V(\{\mathbf{q}_e^r\},\{\mathbf{q}_e^c\})}d\{\mathbf{q}_e^c\}.$$

Here $\{\mathbf{q}_e^r\}$ and $\{\mathbf{q}_e^c\}$ are respectively the local repatoms defining element e and the constrained atoms within this element. More precisely, the contribution of each element is taken equal to that of an infinite crystal undergoing a uniform deformation characterized by the deformation gradient $\mathbf{F}_e$ calculated from the displacements of the repatoms delimiting the element. For completeness and computational efficiency, we appeal to the local harmonic approximation suggested by LeSar [8, 9] to calculate the energy associated with each element. In this approximation, the CG potential energy can be calculated as

$$V_{\rm CG}\left(\{\mathbf{q}^r\},\beta\right)=\sum_i^{\rm NL}E_i+\sum_e\left[n_eU\left(\mathbf{F}_e\right)+\frac{n_e^c}{2\beta}\ln\frac{\|\mathbf{D}\left(\mathbf{F}_e\right)\|}{\left(2\pi k_{\rm B}T\right)^d}\right]$$

where n_e and n_e^c are respectively the total number of atoms and the number of constrained atoms in the element e. $U\left(\mathbf{F}_e\right)$ and $\|\mathbf{D}\left(\mathbf{F}_e\right)\|$ are respectively the energy and the determinant of the dynamical matrix of an atom embedded in an infinite perfect crystal subject to a uniform deformation gradient $\mathbf{F}_e$.

The Nosé-Poincaré dynamics was implemented in the original version of the QC code that can be downloaded at `www.qcmethod.com`. The simulations are essentially $2D$ with periodic boundary conditions in the out-of-plane direction in order to mimic a $3D$ system. In Fig. 2 we compare the the equilibrium lattice parameter of a defect-free single crystal obtained in the *local* regions with regular MD. The QC method gives similar results to those found using MD with a difference ranging from 0% at 0 K to 0.5% at 1000 K. The degradation of the results with increasing temperature is not surprising as anharmonic effects also increase [9]. The discrepancy between the two models is small relative to the standard deviation of atoms from their equilibrium positions (measured in the MD simulation) which range from 1.5% of the lattice parameter at 200 K to 5% at 1000 K.

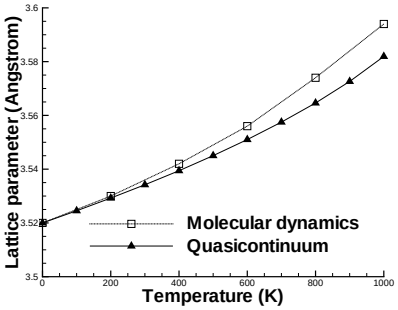

FIG. 2: Lattice parameter of Nickel as a function of temperature using an EAM potential [10]. The QC calculation involved a cell of dimensions 200 nm × 100 nm with a regular mesh containing 50 nodes. The lattice parameter was calculated as an average over the dimensions of the cell.

As a study of the instantaneous behavior of the method, we investigated the temperature dependence for the threshold of dislocation nucleation during nanoindentation. This is an excellent application involving at once localized effects under the indenter and long range effects due to elastic deformation fields. One of the features of nanoindentation experiments that make them especially appealing for multiscale simulations is that the experimental systems remain larger than the biggest cells that can be handled by MD creating a possible source of misinterpretation about the onset of dislocation activity [11]. Previous atomistic simulations have mostly been limited to zero temperature or small system sizes [12–17]. The use of the QC method is therefore compelling since it leads to a reduction in computational overhead that may permit in the future the direct simulation of experimental geometries at finite temperature. In the present work, a single crystal of Ni with dimensions 200 nm × 100 nm was indented by a cylindrical indenter of radius 7 nm at temperatures ranging from 0 K to 400 K (see Fig. 3). The indentation direction coincides with the preferred slip direction $[\bar{1}10]$, the horizontal direction is $[11\bar{1}]$, and the third direction is $[11\bar{2}]$. The mesh used in this simulation was fully-refined beneath the indenter to allow dislocation nucleation and contained about 3000 nodes (compared with 790,000 atoms for full MD). The velocity of the indenter was chosen to be 5 m/s. Nanoindentation simulations were conducted after a 200 ps equilibration time over a period of about 400 ps with a time step of 1 fs. Each simulation was conducted on a standard desktop workstation and required about one day of calculation. The loading curves are presented in Fig. 4. Prior to dislocation nucleation, the curves follow an elastic loading path which is modified by the thermal dependence of the elastic coefficients. As is seen in Fig. 4, the onset

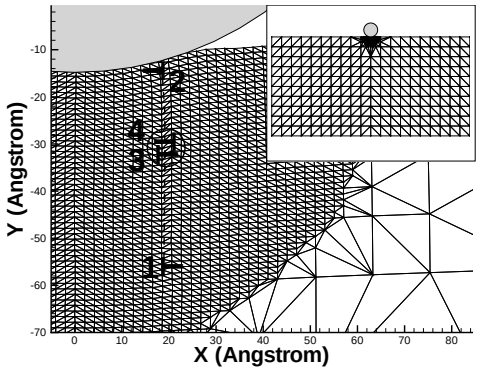

FIG. 3: Computational mesh at an indenter displacement of 1.5 nm at 100 K, showing details of the nonlocal, fully atomistic region under the indenter as a dissociated edge dislocation nucleates. Elements between the repatoms are drawn, rather than the repatoms at the element vertices, to accentuate the deformation due to dislocation motion. Dislocation nucleation occurs in two stages. A first dipole of $\frac{1}{6}\langle 112\rangle$ Shockley partial dislocations (SPD's) is nucleated under the surface (1 and 2). SPD 1 propagates into the bulk while SPD 2 reaches the surface, creating a stacking fault between them as shown by the dashed line. Later a second dipole of SPD's (3 and 4) is nucleated at the same location as the first dipole. SPD 3 propagates into the bulk to form a dissociated dislocation with SPD 1. SPD 4 moves to the surface, removing the stacking fault, and creating a step on the surface by combining with SPD 2. As temperature increases this mechanism occurs closer to the surface and on planes closer to the midline. The inset shows the entire initial mesh.

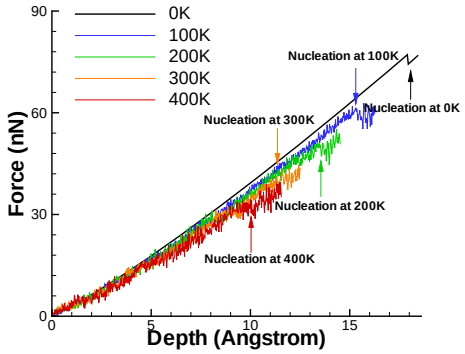

FIG. 4: Force vs indentation depth curve. The forces are averaged over a period of 0.5 ps to reduce thermal noise. The slope decreases with increasing temperature in accordance with the evolution of elastic coefficients. More interestingly, dislocation nucleation occurs at lower displacements with increasing temperature.

of plasticity (i.e. dislocation nucleation) is affected by the temperature. Analysis shows that nucleation occurs under the indenter in the bulk in two stages as presented in Fig. 3. A more comprehensive study will be published elsewhere. We note that the zero temperature results recover earlier results using the QC method in the absence of thermal effects [13].

In this paper we have proposed a method for the dynamical simulation of crystalline solids at constant temperature. It captures both atomistic mechanisms and long range effects without the computational cost of full atomistic simulations. We have shown that thermodynamic properties are in good agreement with conventional atomistic simulations. The ability of this method to investigate effects of temperature and defects in real structures has been demonstrated with the example of nanoindentation. Though these results provide an encouraging first step in the direction of MD simulations without all the atoms, there are a variety of interesting issues still to be explored including: how to carry out mesh adaption at finite temperatures, going beyond the local harmonic approximation used to compute the effective potential and application to other problems of interest such as the temperature dependence of fracture.

We are grateful to Art Voter, Rob Rudd, Michael Ortiz, Jarek Knap, Bill Curtin, David Rodney and Noam Bernstein for useful discussions. We gratefully acknowledge the support of CHSSI, CIMMS, MURI. Part of this work was performed under the auspices of the US DOE by University of California, Lawrence Livermore National Laboratory under Contract W-7405-Eng-48.

[1] G. Lu and E. Kaxiras, in *Handbook of Theoretical and Computational Nanotechnology*, edited by M. Rieth and W. Schommers (American Scientific Publisher, 2005).
[2] E. B. Tadmor, M. Ortiz, and R. Phillips, Phil. Mag. A **73**, 1529 (1996).
[3] V. Shenoy, V. Shenoy, and R. Phillips, Mat. Res. Soc. Symp. **538**, 465 (1999).
[4] K. Huang, *Statistical Mechanics* (Wiley, 1987), 2nd ed.
[5] S. Nosé, Molecular Physics **52**, 255 (1984).
[6] S. D. Bond, B. J. Leimkuhler, and B. B. Laird, J. Comp. Physics **151**, 114 (1999).
[7] M. Tuckerman, B. J. Berne, and G. J. Martyna, J. Chem. Phys. **97**, 1990 (1992).
[8] R. LeSar, R. Najafabadi, and D. J. Srolovitz, Phys. Rev. Lett. **63**, 624 (1989).
[9] S. M. Foiles, Phys. Rev. B **49**, 14930 (1994).
[10] J. Angelo, N. Moody, and M. Baskes, Model. Simul. Mater. Sci. Eng. **3**, 289 (1995).
[11] J. Knap and M. Ortiz, Phys. Rev. Lett. **90**, 226102 (2003).
[12] C. L. Kelchner, S. J. Plimpton, and J. C. Hamilton, Phys. Rev. B **58**, 11085 (1998).
[13] E. B. Tadmor *et al.*, J. Mater. Res. **14**, 2233 (1999).
[14] O. R. de la Fuente *et al.*, Phys. Rev. Lett. **88**, 36101 (2002).
[15] J. Li *et al.*, Nature **418**, 307 (2002).
[16] E. T. Lilleodden *et al.*, J. Mech. Phys. Solids **51**, 910 (2003).
[17] J.-Y. Hsieh *et al.*, Phys. Rev. B **70**, 195424 (2004).